Vol. 107: 151–160, 2013
doi: 10.3354/dao02675

DISEASES OF AQUATIC ORGANISMS
Dis Aquat Org

Published December 12

Retroperitoneal hemangiosarcoma in a common carp *Cyprinus carpio*: a case report

Michael W. Hyatt[1,4,*], Tonya M. Clauss[1], Sophie E. Dennison[2], Alvin C. Camus[3]

[1]Georgia Aquarium, 225 Baker Street, Atlanta, Georgia 30313, USA
[2]Marine Mammal Radiology, 851 Indiana street #307, San Francisco, California 94107, USA
[3]Department of Pathology, University of Georgia, College of Veterinary Medicine, Athens, Georgia 30602, USA

[4]*Present address:* Adventure Aquarium, 1 Riverside Dr., Camden, New Jersey 08103, USA

ABSTRACT: A 7.5 kg common carp *Cyprinus carpio* presented with prominent localized swelling in the caudal right coelomic area, identified by ultrasound as a fluid filled mass. Fine needle aspirate (FNA) and culture results suggested a sterile seroma. Centesis removed 290 ml of serosanguinous fluid that returned within days. Recheck ultrasonography revealed a solid component within the cavity. Radiography demonstrated irregular lysis and misalignment of vertebrae adjacent to the mass, most suggestive of bacterial osteitis or neoplasia. Treatment with antibiotics followed for 2 mo but failed to resolve the lesion. Repeated radiography and ultrasonography showed progressive enlargement of the mass, with vertebral lysis and invasion characteristic of neoplasia. Ultrasound-guided FNA of the solid component of the mass was non-diagnostic. Euthanasia was elected due to the poor clinical response and primary differential of neoplasia. Post-mortem MRI and CT confirmed a retroperitoneal soft tissue mass, partially surrounded by a fluid-filled cavity, causing vertebral lysis and infiltration of the spinal canal. Expansion of the mass caused severe muscle loss and an associated elevation in creatine kinase (>120 000 U l^{-1}). Necropsy results corroborated the MRI and CT findings, revealing a retroperitoneal, multilobular, red and tan mass causing dorsal displacement of the vertebral column, with vertebral lysis, pathologic fracture and invasion of the spinal canal. Histopathologic examination revealed a locally aggressive neoplasm exhibiting multiple patterns of growth, including endothelial lined vascular channels and solid areas formed by more pleomorphic polygonal and spindle cells, consistent with hemangiosarcoma.

KEY WORDS: Hemangiosarcoma · Carp · *Cyprinus carpio* · Ultrasonography · MRI · CT

INTRODUCTION

As fish are living longer under human care due to improved husbandry practices, better technology and progressive veterinary care, spontaneous neoplasia is being reported more frequently. Fish are also being increasingly used as laboratory models of carcinogenesis and as sentinels of environmental pollution. For more detailed information, readers are referred to the review of neoplasia in fishes by Groff (2004).

Cases of vascular neoplasia in fish have been compiled in reviews by Wellings (1969) and Mawdesley-Thomas (1975). Additional cases can be found in the Registry of Tumors for Lower Animals (Harshbarger 1965–1981). Specific examples in fish include hemangioma, hemangioendothelioma and hemangiosarcoma, representing a spectrum of benign, intermediate and malignant tumors of vascular endothelial cells. Hemangiopericytomas, also reported in fish, are a perivascular mesenchymal tumor of contractile pericytes associated with the walls of capillaries and venules (Weiss & Goldblum 2001a).

More recent reports include hemangiomas in scamp *Mycteroperca phenax* (Fournie et al. 1985)

*Email: mhyatt@adventureaquarium.com

and rainbow trout *Oncorhynchus mykiss* (Meyers & Hendricks 1983), hemangiopericytoma in a goldfish *Carassius auratus* (Morales & Schmidt 1991) and an epizootic of cardiac hemangiomas, hemangioendotheliomas and hemangioendotheliosarcomas in the mangrove killifish *Kryptolebias marmoratus* (formerly *Rivulus marmoratus*) (Couch 1995). Both hemangiomas and hemangiosarcomas have been induced in laboratory zebrafish *Danio rerio* experimentally exposed to the carcinogens 7,12 dimethylbenz[a]anthracene (Spitsbergen et al. 2000a) and *N*-methyl-*N′*-nitro-*N*-nitrosoguanidine (Spitsbergen et al. 2000b). Ethylnitrosourea may also have induced cavernous hemangiomas in zebrafish (Beckwith et al. 2000). To the best of our knowledge, the present work is the first report of hemangiosarcoma in the common carp.

CASE REPORT

A 7.5 kg, 66 cm, male common carp *Cyprinus carpio* of unknown age presented in October 2010 for a large, focal swelling in the right coelomic area and erratic swimming (Fig. 1). The fish was housed in a 44 200 gallon freshwater river exhibit and had no prior medical history. It had been acquired 5 yr earlier from the US Fish and Wildlife Service's Warm Springs National Fish Hatchery (Warm Springs, GA, USA), where it was exhibited in a display pool for an unknown period of time.

The carp was anesthetized in 90 mg l^{-1} tricaine methanesulfonate (MS-222, Finquel®, Argent Chemical Laboratories) buffered with 180 mg l^{-1} sodium bicarbonate. On physical examination, a firm, nonmovable, 12 cm focal swelling was present on the right lateral trunk in the area of the caudal coelom. Ultrasonography of the swelling using a portable ultrasound and 5–2 MHz curvilinear probe (Sonosite) revealed an ~10 cm in diameter, irregular, anechoic, fluid-filled mass that appeared to be associated with the body wall, although a discernible separate capsule was not apparent at the time. Initial differential diagnoses included seroma, trauma, abscess, cyst and neoplasia.

Fig. 1. *Cyprinus carpio*. Right-sided caudal swelling in a common carp upon initial presentation

A total of 290 ml of serosanguinous fluid were aspirated using an 18-gauge 1.5 inch (3.8 cm) needle and extension set. A portion of the fluid was centrifuged to concentrate cells, and a cytology preparation was stained with a Romanowsky-type stain (Dip-Quick®, Jorgensen Laboratories). Partial fluid analysis revealed a total protein of 3.4 g dl^{-1} and hematocrit of 1%. Only degenerate erythrocytes upon a proteinaceous background were present, with no evidence of inflammation, infectious agents or neoplastic cells. Fluid was submitted to the Athens Veterinary Diagnostic Laboratory at the University of Georgia (Athens, GA, USA) for aerobic and anaerobic culture. After negative culture results returned several days later, a working diagnosis of seroma was made.

Ultrasonography performed 1 wk later revealed a limiting capsule and provided better observation of deeper aspects of the fluid filled structure, including a small, round hyperechoic component adjacent to the vertebral column. However, determination of a vertebral or retroperitoneal soft tissue origin could not be made. Repeat ultrasonography performed 2, 4, 8, 10 and 12 wk after the initial examination showed continued expansion of the fluid filled cavity and enlargement of the solid component. The fluid became progressively more echogenic, and the peripheral capsule thickened. Initially round, over time, the solid component became more irregularly shaped and developed hyperechoic outer and hypoechoic inner regions that extended into a vertebral centrum (Fig. 2).

Dorsoventral and left lateral radiographs of the caudal trunk performed at Week 4 showed left ventral displacement of the caudal lobe of the swim bladder and 2 misaligned vertebrae exhibiting areas of lysis and bony proliferation (Fig. 3). The changes were suggestive of bacterial osteitis, although neoplasia could not be ruled out. Repeat radiography performed at 8 and 12 wk showed continued progression of the vertebral lytic and proliferative changes and advancement of the discontinuity of vertebral margins.

Using a 3 ml syringe and 18-gauge 1.5 inch (3.8 cm) needle, whole blood was collected and placed in a lithium heparin blood tube for complete blood counts (CBC) and plasma biochemistries 1, 8 and 10 wk after presentation using a ventral midline approach for venipuncture of the caudal vein (Stoskopf 1993). Total white blood cell (WBC) counts were performed

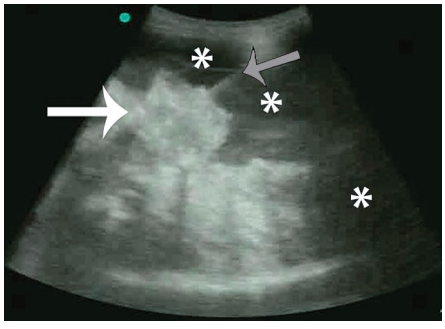

Fig. 2. *Cyprinus carpio*. Ultrasound image of the mixed echogenic soft tissue mass (large white arrow) surrounded by fluid (*). Note the spinal needle (small gray arrow) inserted into the solid component of the mass through the fluid part during the fine needle aspiration. Green dot is the transducer orientation marker

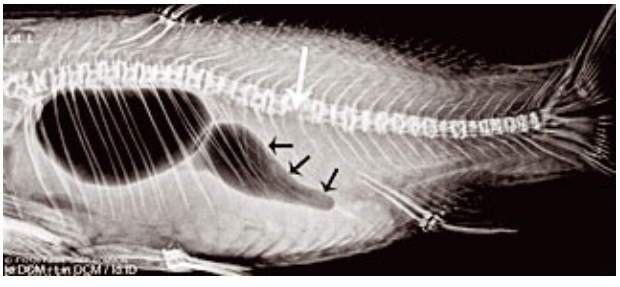

Fig. 3. *Cyprinus carpio*. Left lateral radiograph of the common carp showing vertebral lysis (white arrow) and ventral deviation of the caudal swim bladder (black arrows) caused by the mass

'in-house' using Nat Herrick's diluents (Natt & Herrick 1952) in an improved Neubauer hemacytometer (Bright-Line™, Cambridge Instruments). Air-dried blood smears were stained with Wright's Giemsa (Volu-Sol), and white cell differentials were determined. Total WBC counts, packed cell volumes and plasma proteins were all within normal limits (Saint-Erne 2010). Biochemical analyses were performed by a veterinary reference laboratory (Idexx Reference Laboratories), which included alkaline phosphatase, alanine aminotransferase, aspartate aminotransferase, creatine kinase, gamma-glutamyl transferase, amylase, lipase, albumin, total protein, globulin, total bilirubin, direct bilirubin, indirect bilirubin, blood urea nitrogen, creatinine, cholesterol, glucose, calcium, phosphorus, total carbon dioxide, chloride, potassium, sodium and uric acid. Creatine kinase, normally 4317 to 7392 U l^{-1}, varied from >120 000, to 79 444, to 120 750 U l^{-1} between Weeks 1, 8 and 10, respectively. All other values were within normal limits (Tripathi et al. 2003, Saint-Erne 2010).

An ultrasound-guided FNA of the solid component of the mass was collected after 8 wk using a 20-gauge 3.5 inch (8.9 cm) spinal needle and submitted to the Athens Veterinary Diagnostic Laboratory. Cytologic evaluation of the aspirate revealed only erythrocytes, free nuclei and smudged cells on a proteinaceous background. There was no evidence of neoplastic cells or infectious agents.

Because radiography suggested bacterial osteitis, antibiotic therapy with piperacillin/tazobactam (Zosyn®, Pfizer Animal Health) 100 mg kg^{-1} (via intramuscular injection [i.m.]) every 48 h was initiated 4 wk after presentation. As radiographs showed progressive vertebral lysis after 4 wk of therapy, florfenicol (Nuflor®, Merck Animal Health) 40 mg kg^{-1} i.m. every 48 h was added to the antibiotic regimen. After 8 wk of antibiotic therapy with no evidence of improvement, all treatment was discontinued. As neoplasia was now considered the most likely diagnosis, euthanasia via buffered MS-222 overdose at ~1500 mg l^{-1} was elected 15 wk after initial presentation. Following euthanasia, the fish was taken to Georgia Veterinary Specialists (Sandy Springs, GA, USA) for post-mortem magnetic resonance imaging (MRI) and computed tomography (CT).

MRI (including multiplanar, T1W, T2W and FLAIR) and survey CT (soft tissue and bone reconstruction algorithms) were performed on an Esaote Vet-MR (Universal Medical Systems) and a Picker PQ 2000S CT imaging system (Marconi Medical Systems). At the level of the caudal swim bladder was a predominantly right sided, multilobulated, paravertebral mass that effaced the epaxial and hypaxial paraspinal musculature (Fig. 4A). The mass measured 6.6 × 9.2 × 11.0 cm in size at maximal dimensions. It was mostly fluid attenuating on CT, and on MRI it was T1W isointense to musculature and T2W, T2*W and FLAIR hyperintense to musculature, with signal intensity characteristics on MRI similar to ocular fluid and with fluid attenuation on CT. There was no signal drop out observed on gradient echo (T2*W) sequences (sensitive for certain stages of hemorrhage). The mass invaded and effaced 3 vertebrae and extended into the left and ventral paravertebral tissues. Bone lysis could only be accurately assessed using the CT bone reconstruction algorithm, and vertebral centrum lysis was significant on these images (Fig. 4B). The spinal cord was difficult to evaluate due to limitations of resolution; however, in at least one image, there was extension of the soft tissue component of the mass into the neural canal where it was indistinguishable from the spinal cord. The mass was causing ventral distortion of the right dorsal

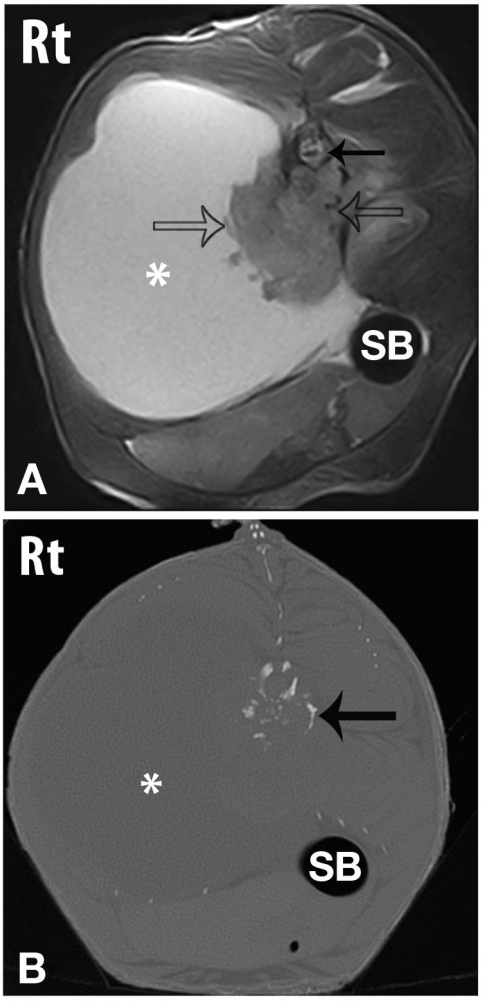

Fig. 4. *Cyprinus carpio*. Transverse MRI and CT images at the same level demonstrating the pathology. The CT and MRI images complement each other to show the complexity of the mass as well as the bone and neural canal involvement. For orientation, the swim bladder (SB) is shown in both images. 'Rt' represents the fish's right side. (A) Transverse T2W MRI image showing the mass with fluid component (*) and solid component (between open arrows) as well as the invasion of bone and the neural canal (black arrow). (B) Transverse CT image (bone reconstruction algorithm displayed with window width 1500, window level 300) showing bone lysis (black arrow) and themass effect (*)

coelomic wall but was not observed to be infiltrating into the coelomic cavity. The combination of imaging findings using the cross-sectional modalities indicated an aggressive disease process, and neoplasia was suspected.

A complete necropsy was performed. The fish was in good physical condition, and autolysis was minimal. The body axis deviated mildly to the right, corresponding to an ~12 cm, unilateral, fluctuant swelling centered on the right side at the lateral line between the pelvic fin and anal fins. The coelomic cavity was opened aseptically from the left side, and samples of caudal kidney, spleen and liver were collected for bacterial culture. The caudal swim bladder was displaced ventrally, but remaining internal organs were grossly unremarkable.

The swelling was formed by a well-delineated, large, cavernous space filled by ~300 ml of clear reddish-brown fluid and limited by a smooth, glistening, variable gray-white lining. There was thinning of overlying skeletal muscle, to which the lining was firmly attached. Located centrally within the cavity, intimately associated with and slightly displacing 2 vertebral bodies dorsally, was a 3 × 4 × 4 cm firm mass, with a friable, uniform tan surface partially rimmed by dark red tissue up to 4 mm thick (Fig. 5A). The mass extended retroperitoneally to form a 7 × 7 × 9 cm multilobular protrusion into the right caudodorsal coelom, immediately caudal to the posterior kidneys. A round, 1.5 cm nodule extended dorsolaterally into skeletal muscle from the vertebral column on the left side. When cut, the surface was reticulated red and white and bordered by a narrow zone of hemorrhage. Bisection of the vertebral column revealed severe osteolysis and presumptive pathologic fracture of 2 vertebral bodies by similar tissue (Fig. 5B) that extended dorsally into the vertebral canal.

A complete set of tissues were collected, fixed in 10% neutral buffered formalin and processed routinely. Histologically, the mass was predominated by extensive areas of coagulative necrosis bordered by neoplastic cells exhibiting multiple patterns of intermingled growth (Fig. 6A). The first growth pattern was characterized by relatively uniform, small, blood filled, vascular channels supported by a scant collagenous stroma. Vascular structures were lined by a single layer of endothelial cells, with small to moderate amounts of pale eosinophilic cytoplasm and plump nuclei that bulged into lumens. Most capillary-like areas were relatively well-differentiated and exhibited only mild cellular pleomorphism. However, in some areas, there was nodular packeting of vessels that had thicker, more disorganized walls, with occasional piling of cells and prominent anisokaryosis (Fig. 6B). Rarely, formative vascular growth produced slightly larger anastomosing channels supported by a minimal collagenous scaffold and lined by spindyloid cells with inconspicuous cytoplasm and small hyperchromatic nuclei that formed luminal projections with a 'hobnail' architecture (Fig. 6C) (Kempson et al. 2001, Warren & Summers 2007).

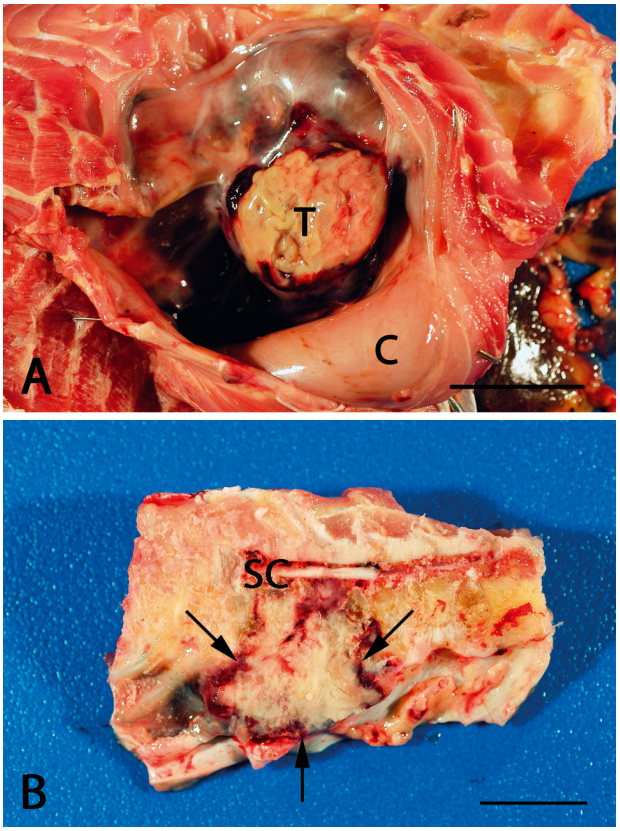

Fig. 5. *Cyprinus carpio*. Gross necropsy images of the carp hemangiosarcoma. (A) Skeletal muscle surrounds a glistening white capsule (C) lining the large fluid filled cavity associated with the centrally located tumor (T). There was extensive necrosis in this portion of the mass. Scale bar = 3 cm. (B) Bisected vertebral column demonstrating vertebral misalignment, osteolysis, and pathologic fracture (arrows) ventral to the spinal cord (SC). Scale bar = 2 cm

These patterns blended or abruptly merged with highly cellular areas formed by variable mixtures of more pleomorphic spindyloid and polygonal cells, with abundant amphophilic cytoplasm and indistinct cell margins. Nuclei varied from irregularly round, to ovoid, to elongate, were euchromatic and vesicular and often possessed a single prominent nucleolus (Fig. 7A). Neoplastic cells grew variably in sheets, in haphazard and streaming arrangements, in short interlacing cords and bundles (Fig. 7B) and in small solid nests. Anisokaryosis was moderate, but large bizarre, including bi-nucleated, forms were occasionally present (Fig. 7C). Mitoses were rare.

Additional features in areas of solid growth included scattered cells with intracytoplasmic lumens (Fig. 8A), some containing eosinophilic globules interpreted as erythrocytes (Fig. 8B). Vascular lumens were infrequent, often cleft-like or tubular and lined by thick, rarely multilayered, endothelial cells. In cross section, these ductal-like formations were reminiscent of adenocarcinoma (Fig. 8C). Small to occasionally moderate mixtures of lymphocytes and plasma cells were scattered throughout, as were small collections of siderophages.

Destruction of vertebral bone by the encroaching neoplasm was extensive, creating a mosaic of osteolysis, pathologic fracture, chondrodysplasia, new bone production and fibrosis. There was infiltration of normal adipose-filled spaces within bone as well as severe lysis characterized by bone with long scalloped margins abutted by tumor and multiple small fragments of bone enveloped by solid neoplastic growth. The neoplasm extended dorsally through a vertebral centrum into the neural canal but did not infiltrate the spinal cord (Fig. 9). The caudal vein was compressed laterally in one section. Infiltration and dissection of perivertebral collagen bundles created ragged peripheral margins.

Lining the fluid filled cavity were 3 to 6 layers of macrophages and multinucleated giant cells. This layer was bordered by a broad zone of loosely organized fibrocollagenous tissue containing large numbers of siderophages. No significant changes were present in other tissues. Bacterial cultures were negative.

DISCUSSION

Microscopic findings in this case were consistent with hemangiosarcoma, a malignant tumor of vascular endothelial cells in humans and other vertebrates (Weiss & Goldblum 2001a, Maxie & Robinson 2007). Spontaneous and chemically induced vascular neoplasms have been reported in wild and laboratory fishes, involving cutaneous sites (Meyers & Hendricks 1983, Fournie et al. 1985, Beckwith et al. 2000) as well as the heart, gills, pharynx, kidney, spleen, peritoneum, mesentery and ocular choroid rete (Couch 1995, Spitsbergen et al. 2000a,b, 2012). However, with the exception of an epizootic of cardiac neoplasms in laboratory reared *Rivulus marmoratus*, histologic descriptions are limited (Couch 1995). Hemangiosarcoma has not been previously reported in the common carp (Harshbarger 1965–1981, Wellings 1969, Mawdesley-Thomas 1975).

In mammals, the microscopic appearance of hemangiosarcomas is often variable and mixed, reflecting different degrees of vascular differentiation. Infiltrative vascular channels lined by variably pleomorphic endothelial cells are usually identifiable somewhere in the mass (Kempson et al. 2001). Piling

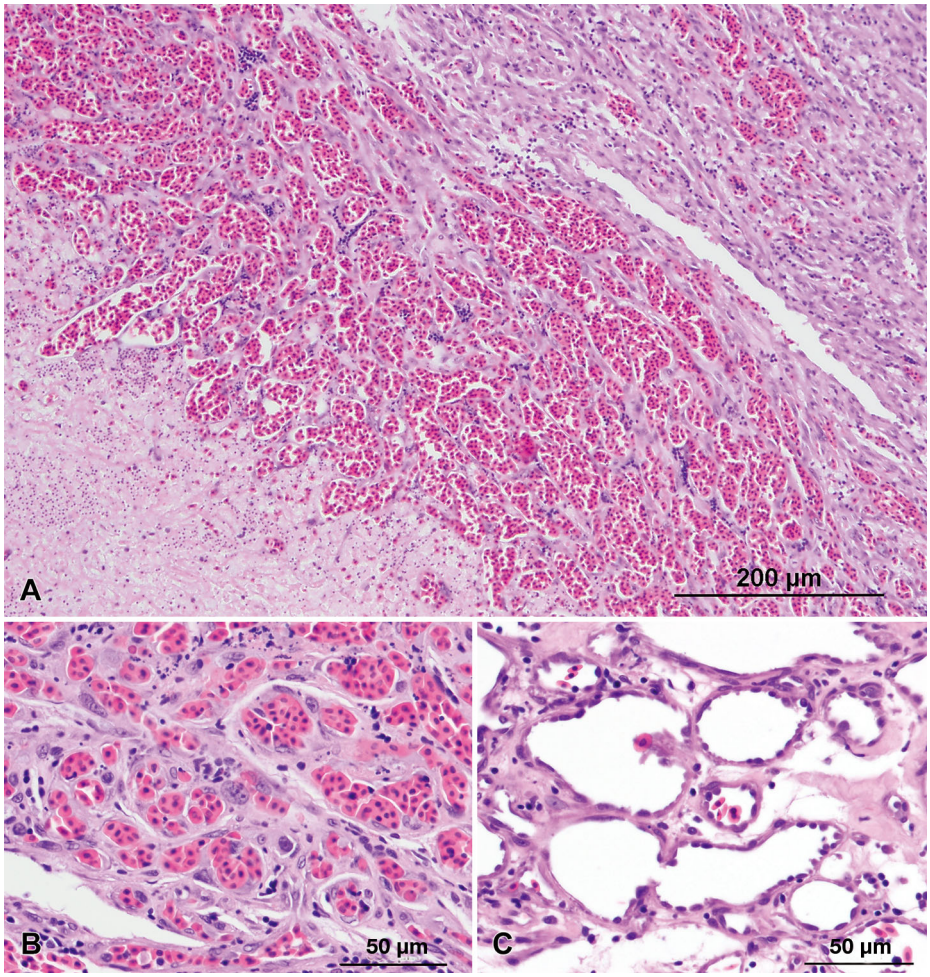

Fig. 6. *Cyprinus carpio*. Photomicrographs of the carp hemangiosarcoma. (A) Low-magnification image of the carp hemangiosarcoma demonstrating primary features of the tumor. Centrally, from upper left to lower right is a broad zone of capillary-like vascular channels that merges abruptly with a region of more solid growth to the upper right. To the lower left, is a pale staining area of necrosis (H&E). (B) Small nodular formations of vascular channels lined by pleomorphic endothelial cells. The center of the field contains a large nucleus with multiple nucleoli (H&E). (C) Delicate vascular channels lined by endothelial cells with inconspicuous cytoplasm and small hyperchromatic nuclei that bulge into lumens in a 'hobnail' fashion (H&E)

of cells, epithelioid morphology, nuclear pleomorphism, nucleolar prominence, increased mitotic index and loss of vasoformative structures are features of malignancy (Gross et al. 2005). Highly anaplastic tumors with closely packed, often spindle shaped, cells can be indistinguishable from fibrosarcomas and other poorly differentiated mesenchymal neoplasms (Kempson et al. 2001, Maxie & Robinson 2007). Hemosiderosis and necrosis are commonly observed (Goldschmidt & Hendrick 2002, Maxie & Robinson 2007).

A progression toward malignancy was observed among 51 tumors in *Rivulus marmoratus*, and considerable variation within and among cases was reported. Hemangiomas were composed of well-differentiated capillary and cavernous vascular channels with patent lumens, while hemangioendotheliomas and hemangiosarcomas had increasingly plump round, polygonal and spindyloid endothelial cells, with fine to vesicular chromatin and prominent nucleoli. In the former, many vessels retained patency, some with luminal endothelial papillary projections. Hemangiosarcomas exhibited greater cellular pleomorphism and prominent areas of disorganized solid growth, with merging of vascular and avascular areas. Nuclei were large and often multilobed, with conspicuous nucleoli. Mitoses were frequent (Couch 1995).

Consistent with the descriptions above, the tumor in this carp exhibited mixed, markedly different growth patterns, ranging from a relatively well-differentiated capillary architecture to highly anaplastic areas composed entirely of spindle cells, and demonstrated numerous additional features of malignancy. However, despite the locally aggressive and highly destructive nature of the tumor, there was little mitotic activity and no evidence of metastasis. For unknown reasons, many fish tumors exhibit fewer signs of malignancy, do not behave as aggressively and metastasize much less frequently compared to their mammalian counterparts (Martineau & Ferguson 2006).

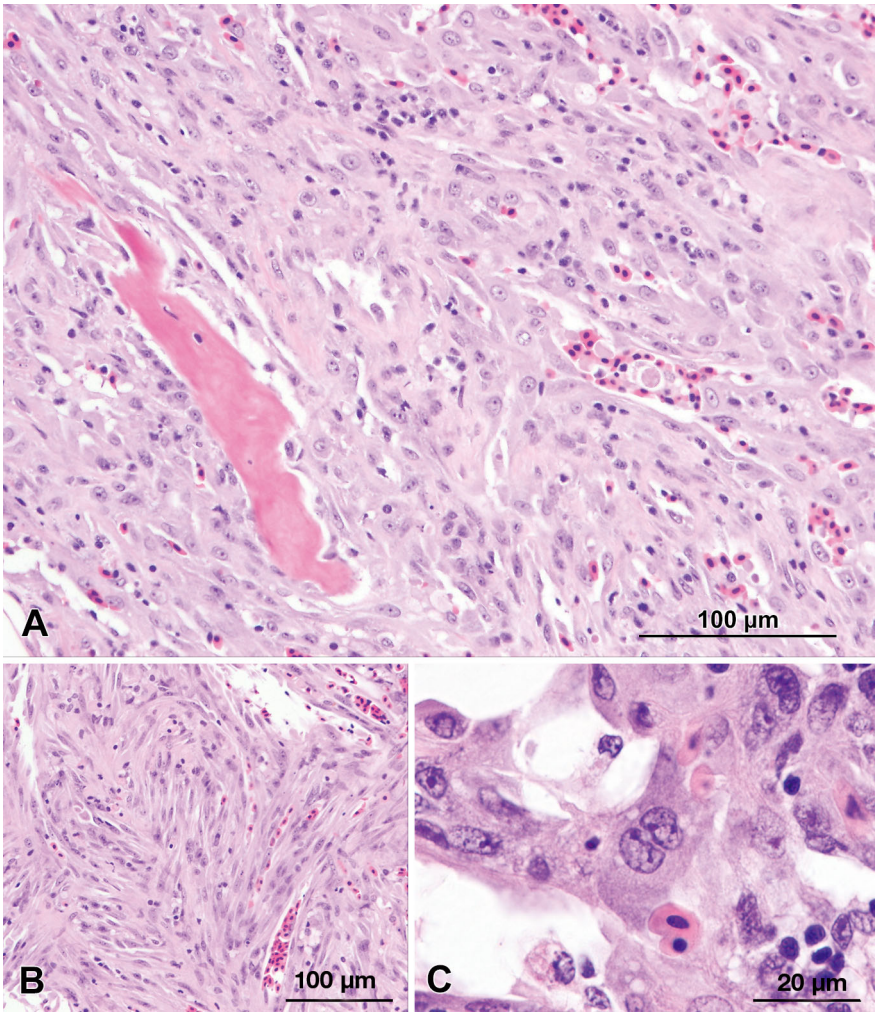

Fig. 7. *Cyprinus carpio*. Photomicrographs of the carp hemangiosarcoma. (A) Fragment of vertebral bone surrounded by a pleomorphic mixture of polygonal and spindyloid cells with indistinct cell margins, abundant amphophilic cytoplasm, large vesicular nuclei and prominent nucleoli (H&E). (B) Area of solid growth composed predominantly of spindle cells arranged in short interlacing bundles that are indistinguishable from other mesenchymal tumors (H&E). (C) Large, polygonal, binucleated cell, with vesicular chromatin and multiple nucleoli (H&E)

Interestingly, the tumor also had features suggestive of the epithelioid (histiocytoid) variant of hemangiosarcoma recognized to arise within deep soft tissue sites, including skeletal muscle, in humans and animals. These features comprised large areas predominated by sheets of large polygonal and plump spindle cells, with amphophilic cytoplasm, large vesicular nuclei, and prominent nucleoli (Fig. 8D). Additional findings included the scattered presence of intracytoplasmic lumens containing erythrocytes and gland-like tubular and ductular structures reminiscent of adenocarcinoma (Kempson et al. 2001, Weiss & Goldblum 2001b, Gross et al. 2005, Warren & Summers 2007).

Immunohistochemical staining (IHC) for the endothelial cell markers, the von Willebrand factor (factor VIII-related antigen) and CD31 (PECAM-1) are useful in the study of endothelial cell-derived neoplasms (Goldschmidt & Hendrick 2002, Maxie & Robinson 2007). However, many canine hemangiosarcomas fail to stain positively for the von Willebrand factor (Goldschmidt & Hendrick 2002). Using the polyclonal rabbit anti-human von Willebrand factor (A0082, Dako) and monoclonal mouse anti-human CD31 (JC70A, Dako) primary antibodies, IHC was attempted. Not unexpectedly, the mammalian antibodies failed to react with carp endothelial cells.

The precise origin of the neoplasm could not be determined, but it likely arose within the paravertebral muscle or connective tissue or within the retroperitoneal space, which contains the kidneys and serves as a conduit for nerves and blood vessels. In dogs, retroperitoneal sarcomas are rare but are most frequently diagnosed as hemangiosarcomas (Liptak et al. 2004). The kidney was not involved and was easily separated from the mass. Destruction of vertebral bone resulted in pathologic fracture. The morphology and physiology of fish bone differs significantly from that of other vertebrates. Spaces and vascular channels exist within some fish bones, but

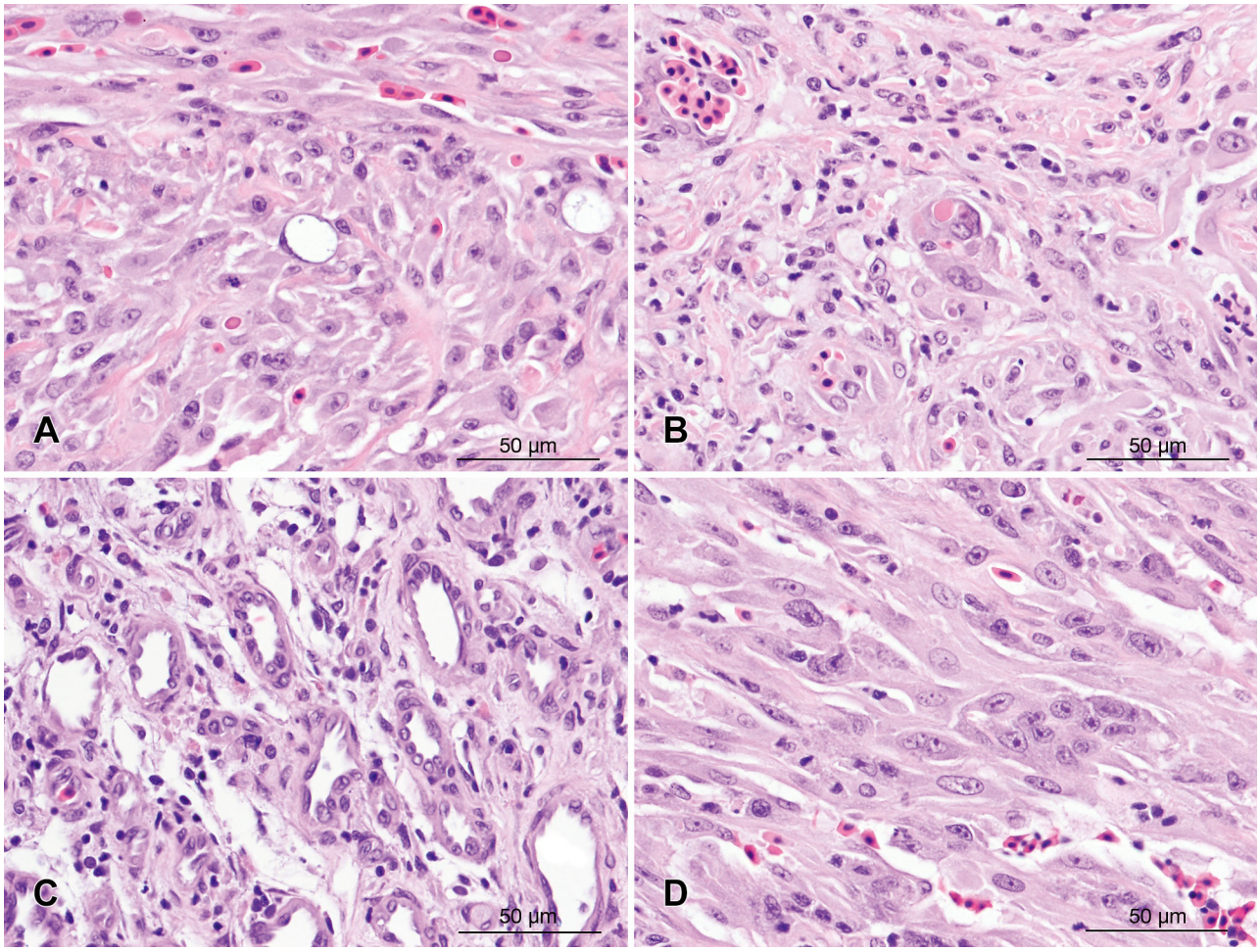

Fig. 8. *Cyprinus carpio*. Photomicrographs of the carp hemangiosarcoma. (A) The cell in the center of the field contains a large intracytoplasmic lumen that displaces the nucleus peripherally in signet ring fashion (H&E). (B) In the center of the field, an intracytoplasmic lumen contains a pale eosinophilic globule suggestive of an erythrocyte (H&E). (C) Portions of the tumor were composed of tubular and ductal-like formations lined by thick endothelial cells reminiscent of adenocarcinoma (H&E). (D) Field of tumor cells with epithelioid and histiocytoid morphology (H&E)

there are no hematopoietic medullary cavities (Roberts & Ellis 2012). Vascular channels may have provided a route for neoplastic invasion, but an origin within bone is considered unlikely.

The unusual fluid filled cavity partially surrounding the mass initially confounded evaluation, leading to an erroneous diagnosis of seroma. Removal of the fluid allowed ultrasonographic visualization of the tumor and the presence of a limiting capsule that thickened over time. Pressure exerted by the enlarging neoplasm is hypothesized to have resulted in atrophy of adjacent muscle, encapsulation and ultimately necrosis in the mass. Fluid accumulation is attributed to hemorrhage, indicated by residual siderophages in the capsule, and leakage from necrotic tissue.

The present report describes an unusual case of retroperitoneal hemangiosarcoma, an uncommon tumor in fish that was previously unknown in carp. Although neoplasia was ultimately suspected, definitive diagnosis required histologic examination. In retrospect, the lack of neoplastic cells in cytologic preparations is not surprising, as hemangiosarcomas are poorly exfoliative (Withrow & Vail 2007). Ultrasonography was essential in following progression of the lesion but was limited by the presence of fluid surrounding the mass. Results of advanced imaging, including MRI and CT, were obtained post-mortem but correlated closely with necropsy findings and demonstrate the utility of cross-sectional imaging in fish medicine. The MRI provided superior soft tissue detail, clearly delin-

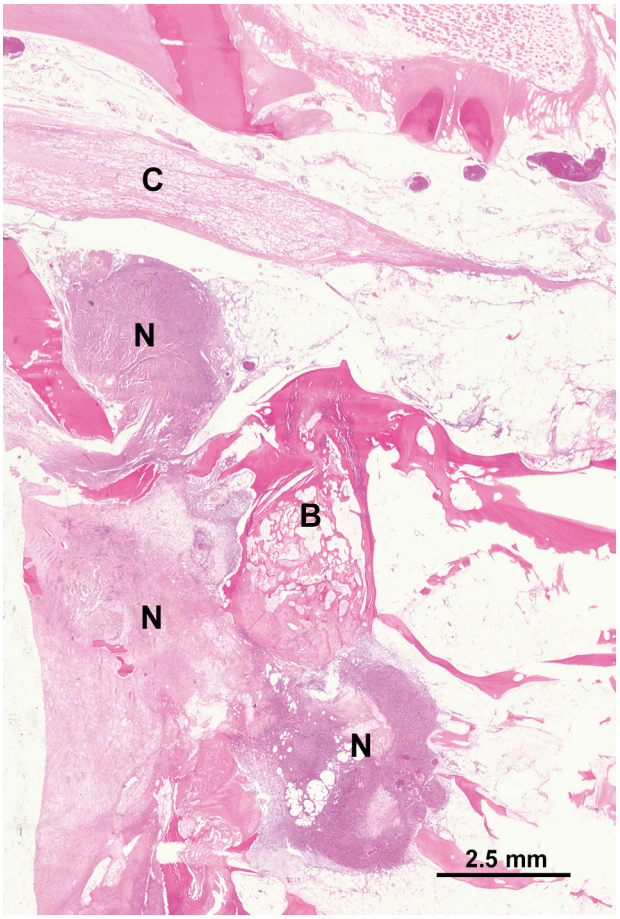

Fig. 9. *Cyprinus carpio*. Subgross image of the carp hemangiosarcoma demonstrating severe destruction and fragmentation of vertebral bone (B) by the infiltrative neoplasm (N). The tumor entered the neural canal but did not invade the spinal cord (C). Scale bar = 2.5 mm

eating fluid from solid areas, while the CT was necessary to demonstrate vertebral lysis. However, work is needed to establish effective restraint and anesthesia methods for use in live animals. In general, complete blood counts and plasma biochemistries provided only minimal diagnostic or prognostic information. However, the lack of a systemic inflammatory response favored neoplasia over an infectious process. Biochemically, elevated creatine kinase levels were consistent with leakage from skeletal muscle adjacent to the mass.

Acknowledgements. We thank the animal care and veterinary staff at the Georgia Aquarium. We also thank Drs. Johnson and Sepulveda and staff from Georgia Veterinary Specialists for the generous donation of services for MRI and CT diagnostic imaging.

LITERATURE CITED

Beckwith LG, Moore JL, Tsao-Wu GS, Harshbarger JC, Cheng KC (2000) Ethylnitrosourea induces neoplasia in zebrafish (*Danio rerio*). Lab Invest 80:379–385

Couch JA (1995) Invading and metastasizing cardiac hemangioendothelial neoplasms in a cohort of the fish *Rivulus marmoratus*: unusually high prevalence, histopathology, and possible etiologies. Cancer Res 55: 2438–2447

Fournie JW, Overstreet RM, Bullock LH (1985) Multiple capillary haemangiomas in the scamp, *Mycteroperca phenax* Jordan and Swain. J Fish Dis 8:551–555

Goldschmidt MH, Hendrick MJ (2002) Tumors of the skin and soft tissues. In: Meuten DJ (ed) Tumors in domestic animals, 4th edn. Iowa State Press, Ames, IA, p 45–118

Groff JM (2004) Neoplasia in fishes. Vet Clin North Am Exot Anim Pract 7:705–756 vii

Gross TL, Ihrke PJ, Walder EJ, Affolter VK (2005) Vascular tumors. In: Walder EJ, Affolter VK (eds) Skin diseases of the dog and cat, clinical and histopathologic diagnosis, 2nd edn. Blackwell Science, Ames, IA, p 735–758

Harshbarger JC (1965–1981) Activities reports. Registry of tumors in lower animals. Smithsonian Institution, Washington, DC

Kempson RL, Fletcher CDM, Evans HL, Hendrickson MR, Sibley RK (2001) Vascular tumors. In: Rosai J (ed) Atlas of tumor pathology, tumors of soft tissues, 3rd Ser, Fascicle 30. Armed Forces Institute of Pathology, Washington, DC, p 307–370

Liptak JM, Dernell WS, Ehrhart EJ, Rizzo SA, Rooney MB, Withrow SJ (2004) Retroperitoneal sarcomas in dogs: 14 cases (1992–2002). J Am Vet Med Assoc 224: 1471–1477

Martineau D, Ferguson HW (2006) Neoplasia. In: Ferguson HW (ed) Systemic pathology of fish, 2nd edn. Scotian Press, London, p 313–335

Mawdesley-Thomas LE (1975) Neoplasia in fish. In: Ribelin WE, Migaki G (eds) The pathology of fishes, 1st edn. The University of Wisconsin Press, Madison, WI, p 805–870

Maxie MG, Robinson WF (2007) Cardiovascular system. In: Maxie MG (ed) Jubb, Kennedy, and Palmer's pathology of domestic animals, Vol 3, 5th edn. Elsevier Saunders, Philadelphia, PA, p 1–106

Meyers TR, Hendricks JD (1983) Histopathology of four spontaneous neoplasms in three species of salmonid fishes. J Fish Dis 6:481–499

Morales P, Schmidt RE (1991) Spindle-cell tumour resembling haemangiopericytoma in a common goldfish, *Carassius auratus* (L.). J Fish Dis 14:499–502

Natt MP, Herrick CA (1952) A new blood diluent for counting the erythrocytes and leucocytes of the chicken. Poult Sci 31:735–738

Roberts RJ, Ellis AE (2012) The anatomy and physiology of teleosts. In: Roberts RJ (ed) Fish pathology, 4th edn. Wiley Blackwell, Chichester, p 17–61

Saint-Erne N (2010) Hematology. In: Saint-Erne N (ed) Advanced koi care, 2nd edn. Erne Enterprises, Glendale, AZ, p 45–46

Spitsbergen JM, Tsai HW, Reddy A, Miller T, Arbogast D, Hendricks JD, Bailey GS (2000a) Neoplasia in zebrafish (*Danio rerio*) treated with 7,12-dimethylbenz[a]anthracene by two exposure routes at different developmental stages. Toxicol Pathol 28:705–715

Spitsbergen JM, Tsai HW, Reddy A, Miller T, Arbogast D, Hendricks JD, Bailey GS (2000b) Neoplasia in zebrafish (*Danio rerio*) treated with *N*-methyl-*N*′-nitro-*N*-nitrosoguanidine by three exposure routes at different developmental stages. Toxicol Pathol 28:716–725

Spitsbergen JM, Buhler DR, Peterson TS (2012) Neoplasia and neoplasm-associated lesions in laboratory colonies of zebrafish emphasizing key influences of diet and aquaculture system design. ILAR J 53:114–125

Stoskopf MK (1993) Clinical examination and procedures. In: Stoskopf MK (ed) Fish medicine. W. B. Saunders, Philadelphia, PA, p 62–78

Tripathi NK, Latimer KS, Lewis TL, Burnley VV (2003) Biochemical reference intervals for koi (*Cyprinus carpio*). Comp Clin Pathol 12:160–165

Warren AL, Summers BA (2007) Epitheliod variant of hemangioma and hemangiosarcoma in the dog, horse, and cow. Vet Pathol 44:15–24

Weiss SW, Goldblum JR (2001a) Malignant vascular tumors. In: Weiss SW, Goldblum JR (eds) Enzinger and Weiss's soft tissue tumors, 4th edn. Mosby, St. Louis, MO, p 917–954

Weiss SW, Goldblum JR (2001b) Perivascular tumors. In: Weiss SW, Goldblum JR (eds) Enzinger and Weiss's soft tissue tumors, 4th edn. Mosby, St. Louis, MO, p 985–1035

Wellings SR (1969) Neoplasia and primitive vertebrate phylogeny: echinoderms, prevertebrates, and fishes — a review. Natl Cancer Inst Monogr 31:59–128

Withrow SJ, Vail DM (2007) Withrow & MacEwen's small animal clinical oncology. Saunders Elsevier, St. Louis, MO

Editorial responsibility: Thomas Lang, Cuxhaven, Germany

Submitted: April 18, 2013; Accepted: September 25, 2013
Proofs received from author(s): December 6, 2013